The evolution of the Hunga hydration in a moistening stratosphere

L. Millán[1], W. G. Read[1], M. L. Santee[1], A. Lambert[1], G. L. Manney[2,3], J. L. Neu[1], M. C. Pitts[4], F. Werner[1], N. J. Livesey[1], M. J. Schwartz[1]

[1]Jet Propulsion Laboratory, California Institute of Technology, Pasadena, California, USA
[2]NorthWest Research Associates, Socorro, New Mexico, USA
[3]New Mexico Institute of Mining and Technology, Socorro, New Mexico, USA
[4]NASA Langley Research Center, Hampton, VA, USA

Key Points:

- The stratospheric water vapor mass has remained essentially unchanged since the Hunga hydration through at least early 2024
- Fueled by excess Hunga water vapor, 2023 Antarctic vortex polar stratospheric cloud dehydration exceeded the climatological mean by ∼50%
- Given its robust (and potentially accelerating) background moistening trend, the stratosphere could stay anomalously humid for years

Corresponding author: L. Millán, `lmillan@jpl.nasa.gov`

Abstract

The 2022 Hunga eruption caused unprecedented stratospheric hydration. Aura Microwave Limb Sounder (MLS) measurements show that the stratospheric water vapor mass remains essentially unchanged as of early 2024 and that the Hunga hydration occurred atop a robust (possibly accelerating) moistening trend in the stratosphere. Enhanced by the excess Hunga water vapor, dehydration via polar stratospheric cloud (PSC) sedimentation in the 2023 Antarctic vortex exceeded climatological values by ∼50%. Simple projections, based solely on Antarctic dehydration, illustrate that the timing of the return to humidity levels that would have been expected absent the Hunga hydration depends on the ongoing stratospheric water vapor trend. For strong moistening, the influx of water entering the stratosphere could offset the enhanced PSC dehydration, resulting in a new, more humid 'equilibrium' stratospheric state. With the Hunga hydration compounding an underlying moistening trend, the stratosphere could remain anomalously humid for an extended period.

Plain Language Summary

The 2022 Hunga eruption injected an unprecedented amount of water vapor directly into the normally very dry stratosphere. This abrupt increase in water vapor from Hunga occurred at a time when the stratosphere was already gradually becoming moister. Using measurements from the Microwave Limb Sounder (MLS) on NASA's Aura satellite, we show that stratospheric water vapor remained elevated, essentially unchanged, from the time of the eruption until at least early 2024. MLS data further reveal that, in 2023, one of the main mechanisms for drying the stratosphere—permanent removal of water vapor by formation and settling of ice polar stratospheric cloud (PSC) particles over Antarctica—was substantially greater than usual, boosted by the excess water vapor from Hunga. Projections indicate that the return to moisture levels that would have been expected in the absence of the eruption depends on how humid the stratosphere continues to get. If moisture levels keep increasing, the extra water vapor entering the stratosphere could balance out the dehydration caused by Antarctic PSCs, leading to a new, more humid equilibrium atmospheric state. Considering the ongoing moistening trend and the water vapor injected by Hunga, the stratosphere could remain unusually humid for a considerable period.

1 Introduction

The importance of stratospheric water vapor (SWV) in Earth's climate system is well established. As a potent greenhouse gas, its radiative forcing affects temperatures locally (e.g., Forster & Shine, 1999) and at the surface (e.g., Solomon et al., 2010). It influences the stratospheric circulation via thermal wind balance (e.g., Maycock et al., 2013) and plays a crucial role in ozone chemistry as the reservoir of odd hydrogen (Evans et al., 1998; Dvortsov & Solomon, 2001; Stenke & Grewe, 2005).

Water vapor enters the stratosphere primarily in the tropics, where tropospheric air freeze-dries at the cold point tropopause (Brewer, 1949), with in-situ methane oxidation providing an additional source of water vapor in the middle-to-upper stratosphere (Jones et al., 1986). The stratosphere is dehydrated primarily by sedimentation of polar stratospheric clouds (PSCs) in the Antarctic polar vortex (Kelly et al., 1989; Fahey et al., 1990; Vömel et al., 1995; Nedoluha et al., 2002; Jiménez et al., 2006) and by transport of stratospheric air into the troposphere in the Brewer-Dobson circulation (BDC) at mid-high latitudes (e.g., Holton et al., 1995; Appenzeller et al., 1996). Much of this transport occurs in stratospheric intrusion events, which are typically associated with decreases in lowermost stratospheric water vapor (e.g., Cox et al., 1997; Škerlak et al., 2015; Schwartz et al., 2015). Another sink of atmospheric water vapor is photodissociation, mainly at mesospheric heights, where the air density is exponentially smaller than in the stratosphere (Nicolet, 1981; Frederick & Hudson, 1980; Nedoluha et al., 2009; Remsberg, 2010).

Interest in SWV and its impacts surged following the eruption of the undersea Hunga volcano (sometimes referred to as Hunga Tonga–Hunga Ha'apai in prior publications). This eruption not only led to the largest perturbation in stratospheric aerosol loading in the last 30 years (e.g., Khaykin et al., 2022; Sellitto et al., 2022; Taha et al., 2022), but also injected ∼150 Tg of water directly into the stratosphere (e.g., Millán et al., 2022; Khaykin et al., 2022; Vömel et al., 2022), instantaneously increasing the SWV mass (SWVm hereafter) by ∼10%.

The eruption impacted stratospheric chemistry (e.g., Evan et al., 2023; Zhu et al., 2023; Santee et al., 2023; Wilmouth et al., 2023). In addition, the radiative forcing from the Hunga water vapor led to unprecedented anomalies in stratospheric and mesospheric temperature and circulation (e.g., Coy et al., 2022; Schoeberl et al., 2022; Sellitto et al., 2022; Yu et al., 2023). The hydration by Hunga also resulted in earlier onset and greater vertical extent of PSCs in the 2023 Antarctic vortex, causing heterogeneous chlorine activation to occur weeks earlier and at higher altitudes than typical (Santee et al., 2024). These observations indicate that the Hunga water vapor plume significantly altered the stratosphere, leaving it in an unprecedented anomalous state. We use water vapor measurements from the Aura Microwave Limb Sounder (MLS; Waters et al., 2006) to analyze the behaviour of SWVm prior to and after the Hunga eruption and to estimate possible future SWVm evolution over the next decade.

2 Datasets and methods

Since its launch in mid-2004, MLS has provided daily profiles of 15 trace gases, including water vapor, as well as temperature and cloud ice, between 82°S and 82°N, offering daily near-global coverage. The substantial enhancement of SWV inside the Hunga plume degraded the accuracy of certain MLS products in the most recent version of MLS data, v5, for around three weeks following the eruption. Consequently, Millán et al. (2022) used v4 data to explore the initial phases of the plume. However, as v5 represents an improvement over v4, particularly for ameliorating water vapor drifts (Livesey et al., 2021), and given our primary focus on SWVm in the years following the eruption, we use v5 MLS data in this study with standard data screening applied (Livesey et al., 2022). An

exception is the period between 15 January and 8 February 2022, during which the Hunga SWV enhancement caused a large proportion of retrievals in the plume to fail the recommended quality screening (Millán et al., 2022). Applying quality screening during this timeframe would result in underestimation of SWVm; thus we used unscreened v5 data through this period. As described in the Supporting Information, we also correct a retrieval artifact in the 10–8 hPa layer (also noted by Niemeier et al., 2023), which is caused by a discontinuity in the a priori used in the MLS retrievals.

SWVm is computed by estimating the partial stratospheric column (i.e., between 100 and 1 hPa) for each MLS profile following the method outlined by Livesey et al. (2006). We then calculate daily zonal mean column amounts, weight them by area, and sum them globally or over specific latitude ranges.

In addition, we use ice PSC volume calculated from measurements by the Cloud-Aerosol Lidar with Orthogonal Polarization (CALIOP; Winker et al., 2009) instrument on the Cloud-Aerosol Lidar and Infrared Pathfinder Satellite Observations (CALIPSO) satellite. PSCs are identified using the CALIOP version 2 detection and composition classification algorithm (Pitts et al., 2018). CALIOP measurements ceased in late June 2023; thus, in 2023 PSCs were measured only during the early part of the Antarctic winter.

Trends are analyzed using a linear (least squares) fit through deseasonalized data, that is, values from which the daily climatological abundances have been removed. We estimate trend uncertainties using a yearly block bootstrap resampling method (Efron & Tibshirani, 1994). Uncertainties derived from block bootstrapping account for autocorrelation of the residuals, thus providing a conservative estimate of those uncertainties (e.g., Bourassa et al., 2014; Froidevaux et al., 2022). We report 2σ uncertainty values (i.e., twice the standard deviations of the bootstrap distributions).

3 Evolution of the Hunga water vapor plume

The movement of the Hunga plume through the stratosphere and mesosphere is shown in Figure 1. We identify the plume location conservatively as regions with 1 ppmv or greater anomaly above the 2005–2021 climatology. The eruption injected water vapor at 20.54°S, 175.38°W throughout most of the vertical extent of the stratosphere. On the day of the eruption, MLS only measured the outer edge of the plume in the upper stratosphere (Figure 1a), where strong winds advected the lofted water vapor to locations sampled by MLS (Millán et al., 2022). Within days (Figures 1b), water vapor injected into the upper stratosphere / lower mesosphere starts to descend towards the mid-stratosphere due to longwave radiative cooling of the upper part of the plume (Sellitto et al., 2022; Niemeier et al., 2023). By a week after the eruption (Figure 1c), the water vapor plume starts to cross the equator, likely due to Rossby waves induced by the excess infrared water vapor cooling (Schoeberl et al., 2023).

For the first three months after the eruption, as the water vapor plume encircles the globe, it slowly broadens latitudinally, spreading mostly northward and remaining essentially confined within the tropical belt (30°S – 30°N, Figures 1a-1e; Millán et al., 2022). Consistent with the seasonal behavior of the BDC (e.g., Lin & Fu, 2013), in the following months the plume spreads southward. Within six months after the eruption, it extends to 60°S but only to 20°N (Figure 1f). By the time the Hunga plume reaches high southern latitudes, the 2022 Antarctic vortex has fully formed, and the transport barrier at its edge effectively prevents the plume from reaching further poleward (Manney et al., 2023).

Around mid-September 2022, the plume begins to rise noticeably in the tropics (Figure 1g; Basha et al., 2023). After 10 months, i.e., mid-November, the plume reaches 82°S, the southernmost point sampled by MLS; the southern polar region is then flooded with Hunga-hydrated air after the breakup of the vortex in December (Manney et al., 2023). Addi-

tionally, the plume continues moving upward in the tropics and starts spreading northward again (Figure 1h) as the Northern Hemisphere cell of the BDC becomes dominant.

A year after the eruption (Figure 1i), Hunga-hydrated air masses have mostly exited the tropical lower stratosphere, driven upward by the large-scale circulation. The SWV anomaly extends from ∼20–3 hPa in the tropics and slopes downward with latitude in the Southern Hemisphere, covering ∼50–10 hPa near the South Pole. Similar morphology is developing in the Northern Hemisphere midlatitudes.

By mid-March 2023 (Figure 1j), the bifurcation of the upper branch of the BDC into the two hemispheres ('rabbit ears') becomes evident. By mid-May (Figure 1k), the 2023 Antarctic vortex is fully developed, and the moisture from Hunga results in earlier onset and greater vertical extent of PSC formation than typical. By mid-June (Figure 1l), dehydration (i.e., sedimentation of PSC particles) removes most of the Hunga excess water inside the polar vortex (Santee et al., 2024; Wohltmann et al., 2024). Furthermore, the Hunga humidity rapidly expands in the northern tropical lower mesosphere, covering 1–0.3 hPa.

Just a month later in mid-July (Figure 1m), anomalous SWV covers most of the tropical lower mesosphere (1<p<0.1 hPa); a month after that, it extends across the entire southern and most of the northern lower mesosphere (Figure 1n). Hunga SWV continues to move upward in the tropics, reaching as high as 0.02 hPa by mid-November (Figure 1o). Two years after the eruption, the anomaly has expanded through most of the lower mesosphere, up to 0.007 hPa at southern high latitudes (Figure 1p). Freeze-dried 'young' air entering through the tropical tropopause has effectively filled the tropical stratosphere, with air directly influenced by Hunga residing predominantly at mid-to-high latitudes. The detailed view of the Hunga hydration from MLS measurements provides an excellent test bed for evaluating the representation of the BDC in climate models, where persistent biases in the transport of water vapor through the stratosphere have long posed a challenge (e.g., Keeble et al., 2021).

4 Stratospheric water vapor mass

The evolution of global (82°S–82°N) SWVm over the 19+ years of the MLS record is summarized in Figure 2a. The most prominent feature is the stratospheric hydration by Hunga (e.g., Millán et al., 2022; Khaykin et al., 2022; Vömel et al., 2022), but several other features are apparent. The year-to-year variability in global SWVm spans ∼100 Tg over 2005–2021. Along with this variability, a moistening trend is evident, with earlier years (light green-blues) being drier than later years (darker blues). This is consistent with results from climate models, which project an increase in SWV due to tropospheric warming (Keeble et al., 2021), and with trends seen previously in MLS measurements (Froidevaux et al., 2019; Konopka et al., 2022). For example, SWVm is ∼50 Tg higher in 2022 prior to the Hunga eruption than the 2005 to 2021 climatological mean. SWVm not only remains strongly enhanced in 2022 (orange line; noted also by Wilmouth et al., 2023), but also persists unabated through 2023 and into 2024 (red and dark red lines), even surpassing the 2022 burden by mid-October 2023.

Figures 2b-2c split SWVm into Northern and Southern Hemisphere contributions. Through 2005–2021, the Northern Hemisphere is on average wetter by 20±9.9 Tg than the Southern Hemisphere (Figure 2d). These hemispheric estimates agree with previous assessments (e.g., Douglass & Stanford, 1982; Rosenlof et al., 1997), which computed an asymmetry of 2% of the total burden (versus 1.5±0.7% from the MLS data). As discussed by Rosenlof et al. (1997), this hemispheric asymmetry arises from three factors: (1) Antarctic polar dehydration, (2) a warmer cold point tropopause (causing less freeze-drying of air entering the stratosphere) during Northern Hemisphere summer, when the core of tropical upwelling is northward of the equator, and (3) differences in winter po-

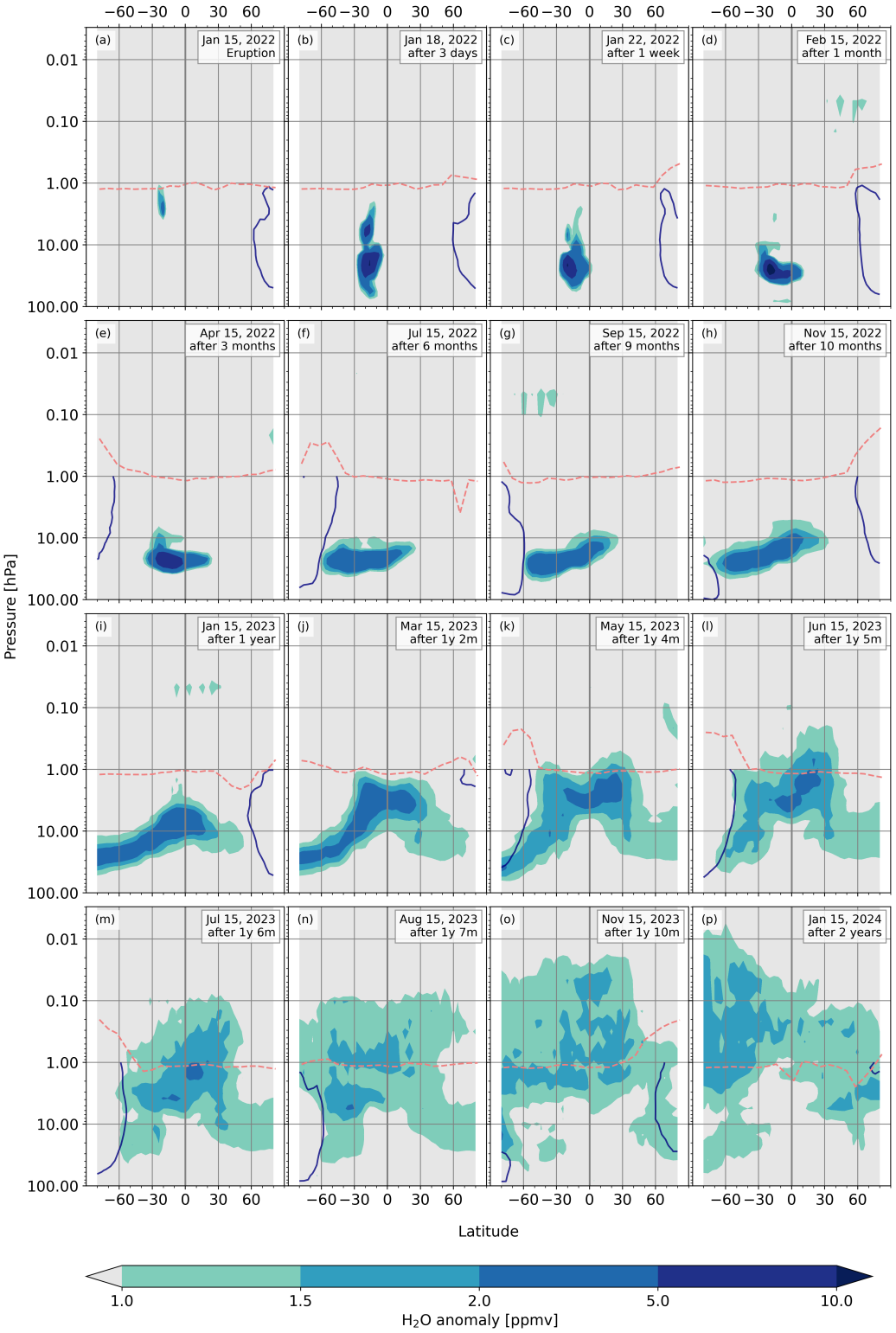

Figure 1. Daily zonal mean water vapor anomalies based on the 2005–2021 monthly climatology for each day. The stratopause, as determined from MLS temperature measurements, is represented by dashed pink lines. Dark blue lines show contours of scaled potential vorticity (see, e.g., Dunkerton & Delisi, 1986; Manney et al., 1994) approximating the stratospheric polar vortex edge region.

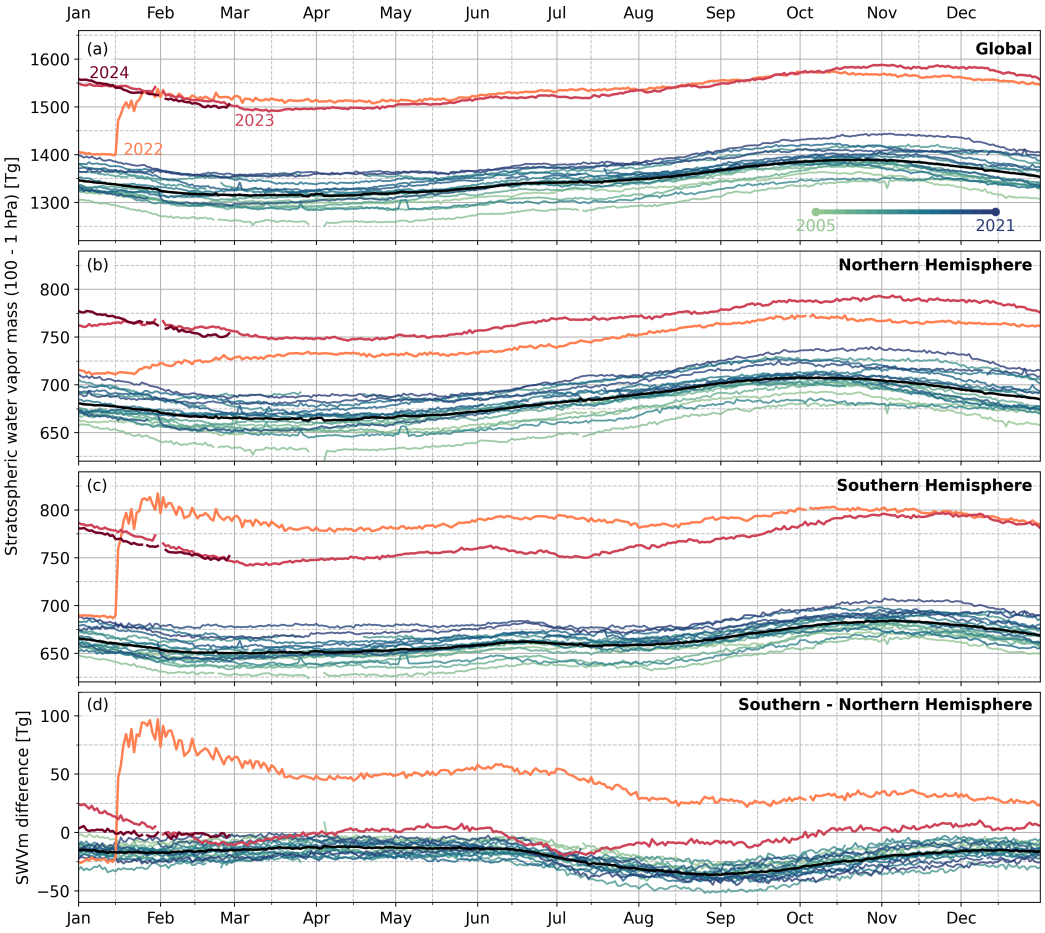

Figure 2. Evolution of the global (a), Northern (b), and Southern (c) Hemisphere SWVm, color-coded by year (see legend), with the 2005–2021 climatology depicted by black lines. (d) The difference between the Northern and Southern Hemisphere SWVm mass. Minor x-ticks are located on the 15th of each month.

lar descent rates. Greater descent in boreal winter leads to more transport of moistened air into the Northern than the Southern Hemisphere.

In 2022, Hunga hydration in the Northern Hemisphere lags behind that in the Southern Hemisphere (Figures 2b-2c), since the volcano injected water at 20.54°S. However, by February 2023, both hemispheres have roughly the same SWVm (Figure 2d). After this date, the hemispheric asymmetry is only 2.5±9.9 Tg (0.2±0.5%). That SWVm remains strongly enhanced into 2024 raises several questions: Will the Hunga water vapor enhancement last 5 to 10 years as hypothesized (Millán et al., 2022; Fleming et al., 2024; Zhou et al., 2024), or will it linger longer in the stratosphere? Is the fact that high SWVm persists in 2024 merely a consequence of prolonged but transient variability acting on top of the Hunga hydration, or does it reflect increasing background values as the stratosphere is becoming moister? How will the apparent upward trend in SWVm affect the return to 'baseline' humidity levels?

5 Stratospheric water vapor mass trends

Figure 3a shows the time series of global deseasonalized daily SWVm anomalies. (To enhance readability, 150 Tg of SWVm from Hunga has been subtracted after January 2022.) Prior to Hunga, the extremes in the global anomalies over the length of the record reach 60 Tg, so the fact that SWVm in late 2023 is slightly larger than that in 2022 could be entirely attributable to SWVm interannual variability. For instance, the SWVm anomaly in 2011 consistently exceeds 20 Tg throughout the year, while in 2021, it consistently exceeds 30 Tg. However, in contrast with the period following Hunga, none of the previous prolonged anomalies remain elevated for longer than a year (Figures 3a, 3b). Moreover, an upward trend over 2005–2021 is discernible, with the stratosphere becoming wetter at a rate of ∼3.7 Tg per year globally, with trends of 2 Tg per year in the Northern and 1.7 Tg per year in the Southern Hemisphere (not shown). These trends agree qualitatively with previously analyzed SWV trends as a function of latitude and altitude, which also show hemispheric asymmetry (Konopka et al., 2022).

The upward trend suggested in Figure 2 is emphasized in Figure 3b, which shows time series of global SWVm (with 150 Tg subtracted after January 2022 as in Figure 3a), along with trends through 2021 estimated starting from different years. The trends remain approximately the same for starting years ranging from 2005 to 2016 (not shown). However, the moistening trend appears to accelerate towards the end of the time series, reaching hydration rates of 7.4 and 13 Tg per year when computed using data starting from 2017 and 2018, respectively, albeit with larger uncertainties than estimated for the trend over the longer 2005–2021 period. As such short-term trends are strongly influenced by decadal variability (e.g., Fueglistaler & Haynes, 2005; Fujiwara et al., 2010; Tao et al., 2023), they are used here only for illustrative purposes.

To investigate whether the moistening trend continues after the Hunga eruption, Figure 3c shows SWVm in the tropics (20°S–20°N), the main point of entry for water vapor into the stratosphere. SWVm essentially returns to pre-eruption levels by early 2023, in agreement with Figure 1l. The evolution throughout the rest of 2023 may indicate a continuation of the strong moistening trend that began around 2017. Comparisons with the trends in the water vapor entering the stratosphere (i.e., water vapor at 100 hPa and 20°S–20°N; e.g., Dessler et al., 2013; Tao et al., 2019), as well as the trends in the MERRA-2 (Modern-Era Retrospective Analysis for Research and Applications Version 2; Gelaro et al., 2017) cold point tropopause temperature in the tropics, support this hypothesis (Figures 3d-3e). Both cold point tropopause temperature and water vapor entry value trends become more positive (i.e., warmer by a factor of 2 and wetter by a factor of 1.4, respectively) and more statistically robust when computed over the period 2005–2023 versus over 2005–2021. Moreover, methane concentrations at the surface have substantially increased in recent years (e.g., Schaefer et al., 2016; Rigby et al., 2017; Nisbet et al., 2019; Zhang et al., 2023), suggesting a corresponding rise in stratospheric water vapor due to methane oxidation. Therefore, the MLS record indicates that the massive enhancement in SWV from Hunga came on top of a strong (and possibly accelerating) moistening trend over the previous 17 years.

6 Antarctic polar vortex dehydration and future stratospheric water projections

Antarctic (82°S–60°S) SWVm (Figure 4a) drops sharply from early June through mid-August every year because of dehydration by PSCs, consistent with the CALIOP-observed PSC season (Figure 4b). The peak-to-valley estimates of seasonal dehydration correlate well with the corresponding integrated ice PSC volumes (Figure 4c), with a correlation coefficient of 0.75 considering all years, or 0.81 neglecting the 2017 austral winter, during which CALIPSO missed more than 30 days in the middle of the season.

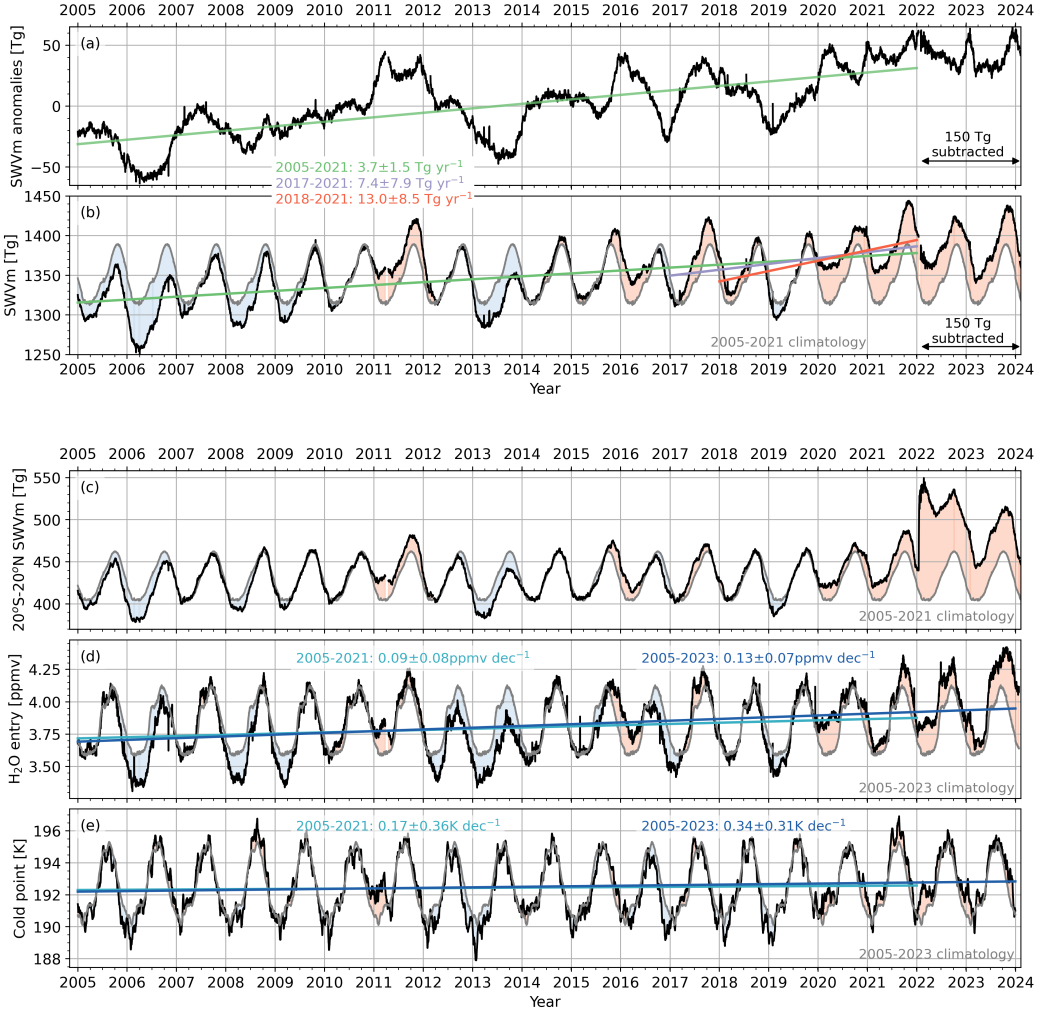

Figure 3. (a) Time series of deseasonalized daily SWVm anomalies from the 2005–2021 climatology, globally and by hemisphere. (b) Time series of daily global SWVm with positive and negative anomalies shaded in red and blue, respectively. Colored lines show trends through 2021 starting in 2005, 2017, and 2018. To extend the plots past January 2022, the 150 Tg of SWVm from Hunga have been subtracted from the anomalies (a) and global SWVm (b). Time series of (c) SWVm in the tropics (20°S–20°N), (d) water vapor entering the stratosphere (at 100 hPa and 20°S–20°N), and (e) the cold point tropopause temperature (20°S–20°N). Colored lines in panels (d) and (e) show trends starting in 2005 through 2021 or 2023; shading in (c)–(e) is as in (b). All trends are reported with 2σ uncertainty values.

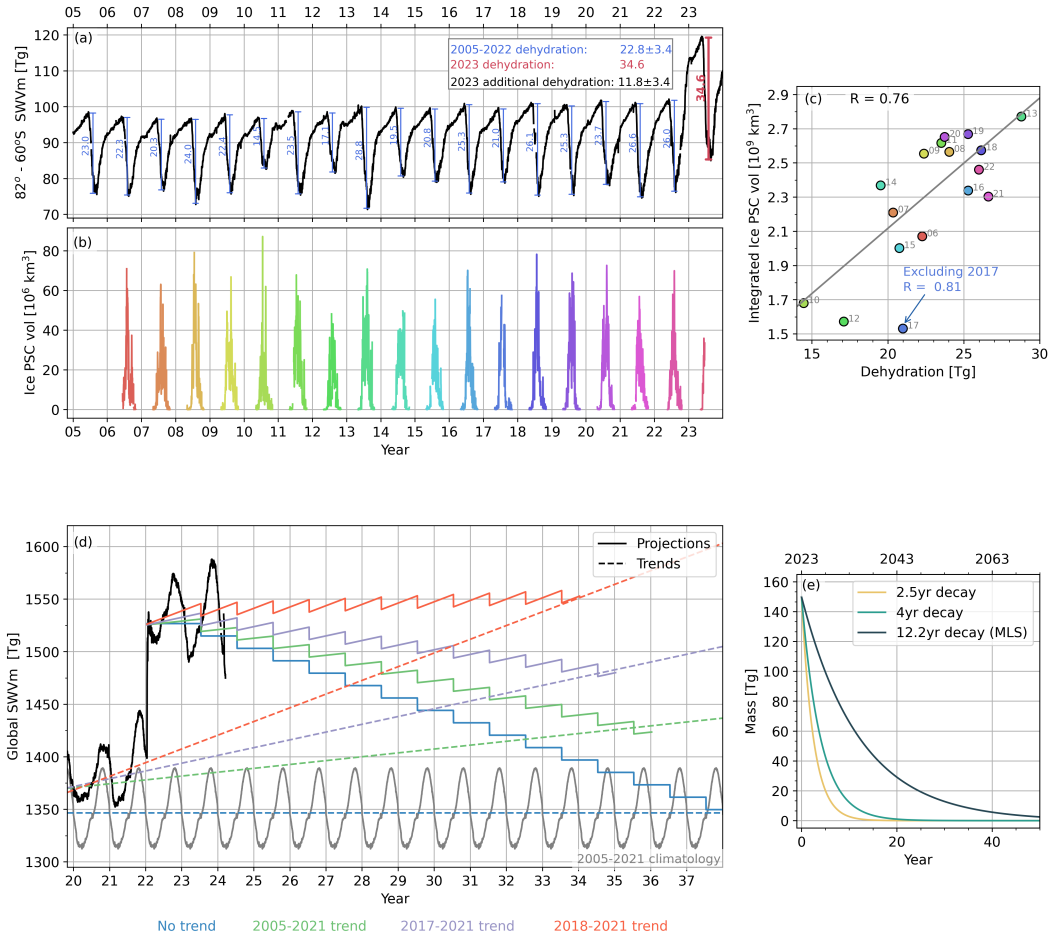

Figure 4. (a) Time series of (a) SWVm in the southern polar region (82°S–60°S), and (b) ice PSC volume color-coded by year. (c) Scatter between dehydration and integrated ice PSC volume. (d) Examples of SWVm projections assuming different background moistening trends and constant dehydration via sedimentation of PSC particles every year. (e) Comparison of exponential decay rates as suggested by models and MLS measurements.

MLS measurements indicate climatological (2005–2022) mean dehydration of 22.8±3.4 Tg per year (as noted earlier, the Hunga water vapor plume was effectively excluded from the 2022 Antarctic polar vortex; Manney et al., 2023). In contrast, the peak-to-valley Antarctic dehydration in 2023 was 34.6 Tg, suggesting that an additional 11.8±3.4 Tg (∼50%) of SWVm was removed through enhanced PSC formation enabled by the excess Hunga water vapor (Santee et al., 2024).

Figure 4d depicts projections of SWVm in upcoming years. These projections naively assume that, as in 2023, an additional 11.8±3.4 Tg of SWVm will continue to be removed from the stratosphere each year via Antarctic dehydration until global SWVm crosses the projected SWV moistening trends, hence reaching the pre-Hunga 'expected' stratospheric moisture. The assumption of constant additional dehydration during each Antarctic winter disregards the likelihood that dehydration will decrease as the excess water vapor from Hunga is removed. Furthermore, this approach overlooks the removal of Hunga water vapor through large-scale downward transport into the troposphere (e.g., Holton

et al., 1995; Appenzeller et al., 1996; Schwartz et al., 2015). (These projections also ignore photolysis in the mesosphere as a sink for water vapor, but it is important to note that the SWVm estimates discussed here exclude the mesosphere.)

The simplicity of these projections notwithstanding, they allow us to discuss hypothetical SWVm future scenarios. Although it is unlikely, the stratosphere could remain in a persistently perturbed state if the strong moistening trend evident over 2018–2021 in the MLS record continues. In this scenario (red line in Figure 4d), the increasing SWVm trend of 13.05 Tg per year would more than counteract the additional 11.8 Tg removed by Antarctic dehydration, leaving the stratosphere in a new, more humid, 'equilibrium' state. With the stratosphere approximately 200 Tg moister than the 2005–2021 climatology, the surface impacts that started with Hunga could become permanent.

Alternatively, assuming the 2017–2021 trend (purple line in Figure 4d), the Hunga water vapor enhancement could last approximately 13±2 years, while under the more moderate and statistically robust 2005–2021 SWV trend (green line), the enhancement could last for around 14±2 years before the stratosphere reverts to its pre-Hunga evolution. In the absence of any SWVm trend (blue line), it would take approximately 16 years to return to 2005–2021 climatological levels. As these hypothetical projections highlight, the return to pre-eruption 'expected' stratospheric humidity hinges on the underlying moisture trend in the stratosphere.

Zhou et al. (2024) identified dehydration by PSCs as the primary removal mechanism of the Hunga water vapor enhancement, constituting over 60% of the total removal in their simulations. Models indicate exponential decay for the excess water vapor, following $y = y_0 e^{(-t/r)}$, where y_0 is the initial anomaly (i.e., ∼150 Tg), r is the decay rate, and t is time in years. So far, model studies have predicted e-folding times of 2.5 (Fleming et al., 2024) or 4 (Zhou et al., 2024) years. Assuming 11.8 Tg dehydration in the first year, MLS data suggest a decay rate of 12.2 years, which results in a removal time for the excess water vapor of more than 50 years (Figure 4e). We emphasize that this projection accounts solely for dehydration by Antarctic PSCs, excluding additional future SWVm losses due to stratospheric intrusions into the troposphere, as well as mesospheric photodissociation. Moreover, this estimate does not account for the half of the Hunga water vapor currently residing in the Northern Hemisphere (Figure 2), which has no substantial SWV sinks (ice PSC formation is very limited in the Arctic) and no efficient transport pathway to the Southern Hemisphere polar region.

7 Conclusions

Two years after the eruption, MLS measurements show that the Hunga water vapor remains at altitudes above (i.e., pressures less than) ∼50 hPa. Hunga-hydrated air masses in the tropical stratosphere have been replaced by the intrusion of 'young' air entering through the tropopause. In addition, the excess moisture has spread throughout most of the lower mesosphere. Nevertheless, the exceptional stratospheric water vapor mass (SWVm) perturbation resulting from the eruption has remained unabated through early 2024.

The lingering elevated SWVm could be attributable to year-to-year variations, since in the past anomalies have exceeded 20 Tg for extended periods (e.g., 2011 and 2021), though never for longer than a year, in contrast to the post-Hunga period. On the other hand, the MLS record indicates that the massive enhancement of SWV from Hunga occurred on top of a robust (and possibly accelerating) moistening trend, which may delay the return to climatological SWVm levels.

MLS measurements show climatological mean dehydration of 22.8 Tg annually through the sedimentation of Antarctic PSCs. However, in 2023, Antarctic PSCs caused dehy-

dration of 34.6 Tg, suggesting that an additional 11.8 Tg (∼50%) of SWVm was eliminated by the enhanced PSC formation fueled by the excess water vapor from Hunga.

Projections of the SWVm based solely on loss via Antarctic dehydration underscore that the timing of the return to the stratospheric humidity levels that would have been expected in the absence of the Hunga eruption hinges on the underlying moistening trend. Assuming, for illustrative purposes, that the 2018–2021 upward trend continues, then the influx of water entering the stratosphere more than offsets the surplus water removed by dehydration through PSC sedimentation, resulting in a new, more humid, 'equilibrium' stratospheric state. Assuming an exponential decay, as indicated by model simulations, MLS measurements suggest a removal time of decades. This estimate considers only Antarctic dehydration and does not account for water vapor loss through large-scale transport to the troposphere or mesospheric photodissociation (processes that are expected to occur eventually). Given that the Hunga stratospheric hydration came atop a robust moistening trend, it seems likely that the stratosphere will remain in an anomalously humid state for decades.

8 Open Research

Aura MLS Level 2 v5 data is publicly available at:
https://disc.gsfc.nasa.gov/datasets?page=1&keywords=AURA%20MLS

Acknowledgments
The research was carried out at the Jet Propulsion Laboratory (JPL), California Institute of Technology, under a contract with the National Aeronautics and Space Administration (80NM0018D0004). GLM was supported by the JPL Microwave Limb Sounder team under JPL subcontract #1521127 to NWRA. We thank L. Froidevaux for helpful discussions.

References

Appenzeller, C., Holton, J. R., & Rosenlof, K. H. (1996). Seasonal variation of mass transport across the tropopause. *Journal of Geophysical Research: Atmospheres*, *101*(D10), 15071–15078. doi: 10.1029/96jd00821

Basha, G., Ratnam, M. V., Kumar, A. H., Jiang, J. H., Babu, S. R., & Kishore, P. (2023). Impact of Hunga Tonga–Hunga Ha'apai volcanic eruption on stratospheric water vapour, temperature, and ozone. *Remote Sensing*, *15*(14), 3602. doi: 10.3390/rs15143602

Bourassa, A. E., Degenstein, D. A., Randel, W. J., Zawodny, J. M., Kyrölä, E., McLinden, C. A., ... Roth, C. Z. (2014). Trends in stratospheric ozone derived from merged SAGE II and Odin-OSIRIS satellite observations. *Atmospheric Chemistry and Physics*, *14*(13), 6983–6994. doi: 10.5194/acp-14-6983-2014

Brewer, A. W. (1949). Evidence for a world circulation provided by the measurements of helium and water vapour distribution in the stratosphere. *Quarterly Journal of the Royal Meteorological Society*, *75*(326), 351–363. doi: 10.1002/qj.49707532603

Cox, B. D., Bithell, M., & Gray, L. J. (1997). Modelling of stratospheric intrusions within a mid-latitude synoptic-scale disturbance. *Quarterly Journal of the Royal Meteorological Society*, *123*(541), 1377–1403. doi: 10.1002/qj.49712354112

Coy, L., Newman, P. A., Wargan, K., Partyka, G., Strahan, S. E., & Pawson, S. (2022). Stratospheric circulation changes associated with the Hunga Tonga–Hunga Ha'apai eruption. *Geophysical Research Letters*, *49*(22). doi: 10.1029/2022gl100982

Dessler, A. E., Schoeberl, M. R., Wang, T., Davis, S. M., & Rosenlof, K. H. (2013). Stratospheric water vapor feedback. *Proceedings of the National Academy of Sciences*, *110*(45), 18087–18091. doi: 10.1073/pnas.1310344110

Douglass, A. R., & Stanford, J. L. (1982). A model of the Antarctic sink for stratospheric water vapor. *Journal of Geophysical Research: Oceans*, *87*(C7), 5001–5008. doi: 10.1029/jc087ic07p05001

Dunkerton, T. J., & Delisi, D. P. (1986). Evolution of potential vorticity in the winter stratosphere of January-February 1979. *Journal of Geophysical Research: Atmospheres*, *91*(D1), 1199–1208. doi: 10.1029/jd091id01p01199

Dvortsov, V. L., & Solomon, S. (2001). Response of the stratospheric temperatures and ozone to past and future increases in stratospheric humidity. *Journal of Geophysical Research: Atmospheres*, *106*(D7), 7505–7514. doi: 10.1029/2000jd900637

Efron, B., & Tibshirani, R. (1994). *An introduction to the bootstrap*. Chapman and Hall/CRC. doi: 10.1201/9780429246593

Evan, S., Brioude, J., Rosenlof, K. H., Gao, R.-S., Portmann, R. W., Zhu, Y., ... Read, W. G. (2023). Rapid ozone depletion after humidification of the stratosphere by the Hunga Tonga Eruption. *Science*, *382*(6668). doi: 10.1126/science.adg2551

Evans, S. J., Toumi, R., Harries, J. E., Chipperfield, M. R., & Russell, J. M. (1998). Trends in stratospheric humidity and the sensitivity of ozone to these trends. *Journal of Geophysical Research: Atmospheres*, *103*(D8), 8715–8725. doi: 10.1029/98jd00265

Fahey, D. W., Kelly, K. K., Kawa, S. R., Tuck, A. F., Loewenstein, M., Chan, K. R., & Heidt, L. E. (1990). Observations of denitrification and dehydration in the winter polar stratospheres. *Nature*, *344*(6264), 321–324. doi: 10.1038/344321a0

Fleming, E. L., Newman, P. A., Liang, Q., & Oman, L. D. (2024). Stratospheric temperature and ozone impacts of the Hunga Tonga–Hunga Ha'apai water vapor injection. *Journal of Geophysical Research: Atmospheres*, *129*(1). doi: 10.1029/2023jd039298

Forster, P. M. d. F., & Shine, K. P. (1999). Stratospheric water vapour changes as a possible contributor to observed stratospheric cooling. *Geophysical Research Letters*, *26*(21), 3309–3312. doi: 10.1029/1999gl010487

Frederick, J. E., & Hudson, R. D. (1980). Atmospheric opacity in the Schumann-Runge bands and the aeronomic dissociation of water vapor. *Journal of the Atmospheric Sciences*, *37*(5), 1088–1098. doi: 10.1175/1520-0469(1980)037⟨1088:aoitsr⟩2.0.co;2

Froidevaux, L., Kinnison, D. E., Santee, M. L., Millán, L. F., Livesey, N. J., Read, W. G., ... Fuller, R. A. (2022). Upper stratospheric ClO and HOCl trends (2005–2020): Aura Microwave Limb Sounder and model results. *Atmospheric Chemistry and Physics*, *22*(7), 4779–4799. doi: 10.5194/acp-22-4779-2022

Froidevaux, L., Kinnison, D. E., Wang, R., Anderson, J., & Fuller, R. A. (2019). Evaluation of CESM1 (WACCM) free-running and specified dynamics atmospheric composition simulations using global multispecies satellite data records. *Atmospheric Chemistry and Physics*, *19*(7), 4783–4821. doi: 10.5194/acp-19-4783-2019

Fueglistaler, S., & Haynes, P. H. (2005). Control of interannual and longer-term variability of stratospheric water vapor. *Journal of Geophysical Research: Atmospheres*, *110*(D24). doi: 10.1029/2005jd006019

Fujiwara, M., Vömel, H., Hasebe, F., Shiotani, M., Ogino, S., Iwasaki, S., ... Oltmans, S. J. (2010). Seasonal to decadal variations of water vapor in the tropical lower stratosphere observed with balloon-borne cryogenic frost point hygrometers. *Journal of Geophysical Research: Atmospheres*, *115*(D18). doi: 10.1029/2010jd014179

Gelaro, R., McCarty, W., Suárez, M. J., Todling, R., Molod, A., Takacs, L., ... Zhao, B. (2017). The Modern-Era Retrospective Analysis for Research and Applications, version 2 (MERRA-2). *Journal of Climate*, *30*(14), 5419–5454. doi: 10.1175/jcli-d-16-0758.1

Holton, J. R., Haynes, P. H., McIntyre, M. E., Douglass, A. R., Rood, R. B., & Pfister, L. (1995). Stratosphere-troposphere exchange. *Reviews of Geophysics*, *33*(4), 403–439. doi: 10.1029/95rg02097

Jiménez, C., Pumphrey, H. C., MacKenzie, I. A., Manney, G. L., Santee, M. L., Schwartz, M. J., ... Waters, J. W. (2006). EOS MLS observations of dehydration in the 2004–2005 polar winters. *Geophysical Research Letters*, *33*(16). doi: 10.1029/2006gl025926

Jones, R. L., Pyle, J. A., Harries, J. E., Zavody, A. M., Russell, J. M., & Gille, J. C. (1986). The water vapour budget of the stratosphere studied using LIMS and SAMS satellite data. *Quarterly Journal of the Royal Meteorological Society*, *112*(474), 1127–1143. doi: 10.1002/qj.49711247412

Keeble, J., Hassler, B., Banerjee, A., Checa-Garcia, R., Chiodo, G., Davis, S., ... Wu, T. (2021). Evaluating stratospheric ozone and water vapour changes in CMIP6 models from 1850 to 2100. *Atmospheric Chemistry and Physics*, *21*(6), 5015–5061. doi: 10.5194/acp-21-5015-2021

Kelly, K. K., Tuck, A. F., Murphy, D. M., Proffitt, M. H., Fahey, D. W., Jones, R. L., ... Heidt, L. E. (1989). Dehydration in the lower Antarctic stratosphere during late winter and early spring, 1987. *Journal of Geophysical Research: Atmospheres*, *94*(D9), 11317–11357. doi: 10.1029/jd094id09p11317

Khaykin, S. M., et al. (2022). Global perturbation of stratospheric water and aerosol burden by Hunga eruption. *Communications Earth & Environment*, *3*. doi: 10.1038/s43247-022-00652-x

Konopka, P., Tao, M., Ploeger, F., Hurst, D. F., Santee, M. L., Wright, J. S., & Riese, M. (2022). Stratospheric moistening after 2000. *Geophysical Research Letters*, *49*(8). doi: 10.1029/2021gl097609

Lin, P., & Fu, Q. (2013). Changes in various branches of the Brewer–Dobson circulation from an ensemble of chemistry climate models. *Journal of Geophysical Research: Atmospheres*, *118*(1), 73–84. doi: 10.1029/2012jd018813

Livesey, N. J., Read, W., Wagner, P. A., Froidevaux, L., Santee, M. L., Schwartz, M. J., ... R., L. R. (2022). *Version 5.0x Level 2 and 3 data quality and description document* (Tech. Rep. No. JPL D-105336 Rev. B). Jet Propulsion Laboratory.

Livesey, N. J., Read, W. G., Froidevaux, L., Lambert, A., Santee, M. L., Schwartz, M. J., ... Nedoluha, G. E. (2021). Investigation and amelioration of long-term instrumental drifts in water vapor and nitrous oxide measurements from the aura microwave limb sounder (mls) and their implications for studies of variability and trends. *Atmospheric Chemistry and Physics*, *21*(20), 15409–15430. doi: 10.5194/acp-21-15409-2021

Livesey, N. J., Van Snyder, W., Read, W., & Wagner, P. (2006). Retrieval algorithms for the EOS Microwave limb sounder (MLS). *IEEE Transactions on Geoscience and Remote Sensing*, *44*(5), 1144–1155. doi: 10.1109/tgrs.2006.872327

Manney, G. L., Santee, M. L., Lambert, A., Millán, L. F., Minschwaner, K., Werner, F., ... Wang, T. (2023). Siege in the southern stratosphere: Hunga Tonga–Hunga Ha'apai water vapor excluded from the 2022 Antarctic polar vortex. *Geophysical Research Letters*, *50*(14). doi: 10.1029/2023gl103855

Manney, G. L., Zurek, R. W., Gelman, M. E., Miller, A. J., & Nagatani, R. (1994). The anomalous Arctic lower stratospheric polar vortex of 1992–1993. *Geophysical Research Letters*, *21*(22), 2405–2408. doi: 10.1029/94gl02368

Maycock, A. C., Joshi, M. M., Shine, K. P., & Scaife, A. A. (2013). The circulation response to idealized changes in stratospheric water vapor. *Journal of Climate*,

26(2), 545–561. doi: 10.1175/jcli-d-12-00155.1

Millán, L. F., et al. (2022). The Hunga Tonga-Hunga Ha'apai hydration of the stratosphere. *Geophys. Res. Lett.*, *49*. doi: 10.1029/2022GL099381

Nedoluha, G. E., Bevilacqua, R. M., & Hoppel, K. W. (2002). POAM III measurements of dehydration in the Antarctic and comparisons with the Arctic. *Journal of Geophysical Research: Atmospheres*, *107*(D20). doi: 10.1029/2001jd001184

Nedoluha, G. E., Gomez, R. M., Hicks, B. C., Wrotny, J. E., Boone, C., & Lambert, A. (2009). Water vapor measurements in the mesosphere from Mauna Loa over solar cycle 23. *Journal of Geophysical Research: Atmospheres*, *114*(D23). doi: 10.1029/2009jd012504

Nicolet, M. (1981). The photodissociation of water vapor in the mesosphere. *Journal of Geophysical Research: Oceans*, *86*(C6), 5203–5208. doi: 10.1029/jc086ic06p05203

Niemeier, U., Wallis, S., Timmreck, C., van Pham, T., & von Savigny, C. (2023). How the Hunga Tonga–Hunga Ha'apai water vapor cloud impacts its transport through the stratosphere: Dynamical and radiative effects. *Geophysical Research Letters*, *50*(24). doi: 10.1029/2023gl106482

Nisbet, E. G., Manning, M. R., Dlugokencky, E. J., Fisher, R. E., Lowry, D., Michel, S. E., ... White, J. W. C. (2019). Very strong atmospheric methane growth in the 4 years 2014–2017: Implications for the Paris Agreement. *Global Biogeochemical Cycles*, *33*(3), 318–342. doi: 10.1029/2018gb006009

Pitts, M. C., Poole, L. R., & Gonzalez, R. (2018). Polar stratospheric cloud climatology based on CALIPSO spaceborne lidar measurements from 2006 to 2017. *Atmospheric Chemistry and Physics*, *18*(15), 10881–10913. doi: 10.5194/acp-18-10881-2018

Remsberg, E. (2010). Observed seasonal to decadal scale responses in mesospheric water vapor. *Journal of Geophysical Research: Atmospheres*, *115*(D6). doi: 10.1029/2009jd012904

Rigby, M., Montzka, S. A., Prinn, R. G., White, J. W. C., Young, D., O'Doherty, S., ... Park, S. (2017). Role of atmospheric oxidation in recent methane growth. *Proceedings of the National Academy of Sciences*, *114*(21), 5373–5377. doi: 10.1073/pnas.1616426114

Rosenlof, K. H., Tuck, A. F., Kelly, K. K., Russell, J. M., & McCormick, M. P. (1997). Hemispheric asymmetries in water vapor and inferences about transport in the lower stratosphere. *Journal of Geophysical Research: Atmospheres*, *102*(D11), 13213–13234. doi: 10.1029/97jd00873

Santee, M. L., Lambert, A., Froidevaux, L., Manney, G. L., Schwartz, M. J., Millán, L. F., ... Fuller, R. A. (2023). Strong evidence of heterogeneous processing on stratospheric sulfate aerosol in the extrapolar southern hemisphere following the 2022 Hunga Tonga–Hunga Ha'apai eruption. *Journal of Geophysical Research: Atmospheres*, *128*(16). doi: 10.1029/2023jd039169

Santee, M. L., Manney, G. L., Lambert, A., Millán, L., Livesey, N. J., Pitts, M. C., ... Fuller, R. (2024). The influence of stratospheric hydration from the Hunga eruption on chemical processing in the 2023 Antarctic vortex. doi: 10.22541/essoar.170542085.55151307/v1

Schaefer, H., Fletcher, S. E. M., Veidt, C., Lassey, K. R., Brailsford, G. W., Bromley, T. M., ... White, J. W. C. (2016). A 21st-century shift from fossil-fuel to biogenic methane emissions indicated by 13 ch 4. *Science*, *352*(6281), 80–84. doi: 10.1126/science.aad2705

Schoeberl, M. R., Wang, Y., Ueyama, R., Taha, G., Jensen, E., & Yu, W. (2022). Analysis and impact of the Hunga Tonga–Hunga Ha'apai stratospheric water vapor plume. *Geophysical Research Letters*, *49*(20). doi: 10.1029/2022gl100248

Schoeberl, M. R., Wang, Y., Ueyama, R., Taha, G., & Yu, W. (2023). The cross equatorial transport of the Hunga Tonga–Hunga Ha'apai eruption plume. *Geophysical Research Letters*, *50*(4). doi: 10.1029/2022gl102443

Schwartz, M. J., Manney, G. L., Hegglin, M. I., Livesey, N. J., Santee, M. L., & Daffer, W. H. (2015). Climatology and variability of trace gases in extratropical double-tropopause regions from MLS, HIRDLS, and ACE-FTS measurements. *Journal of Geophysical Research: Atmospheres*, *120*(2), 843–867. doi: 10.1002/2014jd021964

Sellitto, P., Podglajen, A., Belhadji, R., Boichu, M., Carboni, E., Cuesta, J., ... Legras, B. (2022). The unexpected radiative impact of the Hunga Tonga eruption of 15th January 2022. *Communications Earth & Environment*, *3*(1). doi: 10.1038/s43247-022-00618-z

Solomon, S., Rosenlof, K. H., Portmann, R. W., Daniel, J. S., Davis, S. M., Sanford, T. J., & Plattner, G.-K. (2010). Contributions of stratospheric water vapor to decadal changes in the rate of global warming. *Science*, *327*(5970), 1219–1223. doi: 10.1126/science.1182488

Stenke, A., & Grewe, V. (2005). Simulation of stratospheric water vapor trends: impact on stratospheric ozone chemistry. *Atmospheric Chemistry and Physics*, *5*(5), 1257–1272. doi: 10.5194/acp-5-1257-2005

Taha, G., Loughman, R., Colarco, P. R., Zhu, T., Thomason, L. W., & Jaross, G. (2022). Tracking the 2022 Hunga Tonga–Hunga Ha'apai aerosol cloud in the upper and middle stratosphere using space-based observations. *Geophys. Res. Lett.*, *49*. doi: 10.1029/2022GL100091

Tao, M., Konopka, P., Ploeger, F., Yan, X., Wright, J. S., Diallo, M., ... Riese, M. (2019). Multitimescale variations in modeled stratospheric water vapor derived from three modern reanalysis products. *Atmospheric Chemistry and Physics*, *19*(9), 6509–6534. doi: 10.5194/acp-19-6509-2019

Tao, M., Konopka, P., Wright, J. S., Liu, Y., Bian, J., Davis, S. M., ... Ploeger, F. (2023). Multi-decadal variability controls short-term stratospheric water vapor trends. *Communications Earth & Environment*, *4*(1). doi: 10.1038/s43247-023-01094-9

Vömel, H., Evan, S., & Tully, M. (2022). Water vapor injection into the stratosphere by Hunga Tonga–Hunga Ha'apai. *Science*, *377*, 1444–1447. doi: 10.1126/science.abq2299

Vömel, H., Oltmans, S. J., Hofmann, D. J., Deshler, T., & Rosen, J. M. (1995). The evolution of the dehydration in the Antarctic stratospheric vortex. *Journal of Geophysical Research: Atmospheres*, *100*(D7), 13919–13926. doi: 10.1029/95jd01000

Waters, J., Froidevaux, L., Harwood, R., Jarnot, R., Pickett, H., Read, W., ... Walch, M. (2006). The Earth Observing System Microwave Limb Sounder (EOS MLS) on the Aura satellite. *IEEE Transactions on Geoscience and Remote Sensing*, *44*(5), 1075–1092. doi: 10.1109/tgrs.2006.873771

Wilmouth, D. M., Østerstrøm, F. F., Smith, J. B., Anderson, J. G., & Salawitch, R. J. (2023). Impact of the Hunga Tonga volcanic eruption on stratospheric composition. *Proceedings of the National Academy of Sciences*, *120*(46). doi: 10.1073/pnas.2301994120

Winker, D. M., Vaughan, M. A., Omar, A., Hu, Y., Powell, K. A., Liu, Z., ... Young, S. A. (2009). Overview of the CALIPSO mission and CALIOP data processing algorithms. *Journal of Atmospheric and Oceanic Technology*, *26*(11), 2310–2323. doi: 10.1175/2009jtecha1281.1

Wohltmann, I., Santee, M. L., Manney, G. L., & Millán, L. F. (2024). The chemical effect of increased water vapor from the Hunga Tonga–Hunga Ha'apai eruption on the Antarctic ozone hole. *Geophysical Research Letters*, *51*(4). doi: 10.1029/2023gl106980

Yu, W., Garcia, R., Yue, J., Smith, A., Wang, X., Randel, W., ... Mlynczak, M. (2023). Mesospheric temperature and circulation response to the Hunga Tonga–Hunga-Ha'apai volcanic eruption. *Journal of Geophysical Research: Atmospheres*, *128*(21). doi: 10.1029/2023jd039636

Zhang, Z., Poulter, B., Feldman, A. F., Ying, Q., Ciais, P., Peng, S., & Li, X. (2023). Recent intensification of wetland methane feedback. *Nature Climate Change*, *13*(5), 430–433. doi: 10.1038/s41558-023-01629-0

Zhou, X., Dhomse, S. S., Feng, W., Mann, G., Heddell, S., Pumphrey, H., ... Chipperfield, M. P. (2024). Antarctic vortex dehydration in 2023 as a substantial removal pathway for Hunga Tonga–Hunga Ha'apai water vapour. doi: 10.22541/essoar.170603848.83725516/v1

Zhu, Y., Portmann, R. W., Kinnison, D., Toon, O. B., Millán, L., Zhang, J., ... Rosenlof, K. H. (2023). Stratospheric ozone depletion inside the volcanic plume shortly after the 2022 Hunga Tonga eruption. *Atmospheric Chemistry and Physics*, *23*(20), 13355–13367. doi: 10.5194/acp-23-13355-2023

Škerlak, B., Sprenger, M., Pfahl, S., Tyrlis, E., & Wernli, H. (2015). Tropopause folds in era-interim: Global climatology and relation to extreme weather events. *Journal of Geophysical Research: Atmospheres*, *120*(10), 4860–4877. doi: 10.1002/2014jd022787